

# SURFACE, INTERFACE AND THIN FILM ANALYSIS IN MATERIAL SCIENCE

Helmut Viefhaus  
Max-Planck-Institut für Eisenforschung GmbH  
40237 Düsseldorf, Germany

## INVITED PAPER

22<sup>nd</sup> International Conference on Microelectronics, MIEL'94  
30<sup>th</sup> Symposium on Devices and Materials, SD'94  
September 28. - September 30., 1994, Rogla, Slovenia

**Keywords:** material science, surface phenomena, interface layers, industrial applications, thin films, surface analysis, electron diffraction, Low Energy Electron Diffraction, Scanning Tunnelling Microscopy, Auger Electron Spectroscopy, Secondary Ion Mass Spectroscopy, X-ray Photoelectron Spectroscopy, Secondary Neutrals Mass Spectrometry, material interaction

**Abstract:** Surface phenomena and processes occurring at interfaces play an important role in a variety of industrial applications and an ever growing need for surface characterization allowing better understanding of the processes can be observed.

After giving a short definition of a surface of a solid, some of the main surface analytical methods like LEED Low energy electron diffraction, STM Scanning tunneling microscopy, AES Auger electron spectroscopy, XPS X-Ray photo electron spectroscopy, and SIMS Secondary ion mass spectroscopy are briefly discussed.

The main surface phenomena which can change the chemical composition of surfaces are adsorption from the surrounding gas phase and segregation of atoms from the bulk at elevated temperatures. Some theoretical considerations and illustrating examples of experimental studies on those phenomena will be presented.

## Analiza površin, meja in tankih plasti v materialoznanstvu

**Ključne besede:** znanost o materialih, pojavi površinski, sloji vmesni, aplikacije industrijske, plasti tanke, analiza površine, difrakcija elektronska, LEED difrakcija elektronov energije nizke, STM mikroskopija skenirna tunelna, AES Auger spektroskopija Elektronska, SIMS spektroskopija masna z ioni sekundarnimi, XPS spektroskopija fotoelektronska z X-žarki, SNMS spektrometrija masna z nevtrali sekundarnimi, vplivanje med materiali

**Povzetek:** Pojavi, ki se dogajajo na površini in na meji med površinama, postajajo vse bolj in bolj pomembni v različnih industrijskih vejah, saj lahko opazimo stalen porast zanimanja za karakterizacijo površine, ki omogoča boljše razumevanje procesov na površini.

Kratki definiciji površine trdne snovi sledi opis nekaterih glavnih analitičnih metod za karakterizacijo površine, kot so: LEED-Low Energy Electron Diffraction, STM - Scanning Tunnelling Microscopy, AES-Auger Electron Spectroscopy, XPS-X-ray Photo Electron Spectroscopy in SIMS-Secondary Ion Mass Spectroscopy.

Pomembna površinska pojava, ki lahko spremenita kemično sestavo površin, sta adsorpcija iz okolišnega plina in segregacija atomov iz notranjosti snovi pri povišani temperaturi. V referatu predstavljam nekaj teoretičnih izhodišč, kakor tudi ilustrativne eksperimentalne rezultate teh fenomenov.

### Introduction

As every material interacts by its surface with the environment, the surface will be different from the material beneath it. But even if a clean surface of a solid would be created within an extremely good vacuum bonding imbalances for the atoms exist for the outermost atomic layers and they induce very special surface properties. By those surface properties on the other hand, many phenomena in material science are affected, some of those phenomena are listed in table 1.

The surface of a solid metal may be defined by the termination of the bulk state, where the symmetry of the bulk is disturbed to give altered interaction forces in this region. As a consequence of the bonding imbalances at the surface the structure of the outermost atomic layers may change in comparison to the bulk structure, this is schematically illustrated in fig. 1. The first example,

shown in fig. 1a, may be an acceptable model for so-called "sheet" structures like graphite for example which exhibits only weak dispersion forces between the individual atomic layers. For a strong bonding between the atomic layers the breakdown of balanced bonding

- corrosion
- catalysis
- adhesion
- wear
- joining
- inhibition
- passivation
- sintering
- a.s.o.

TABLE - 1

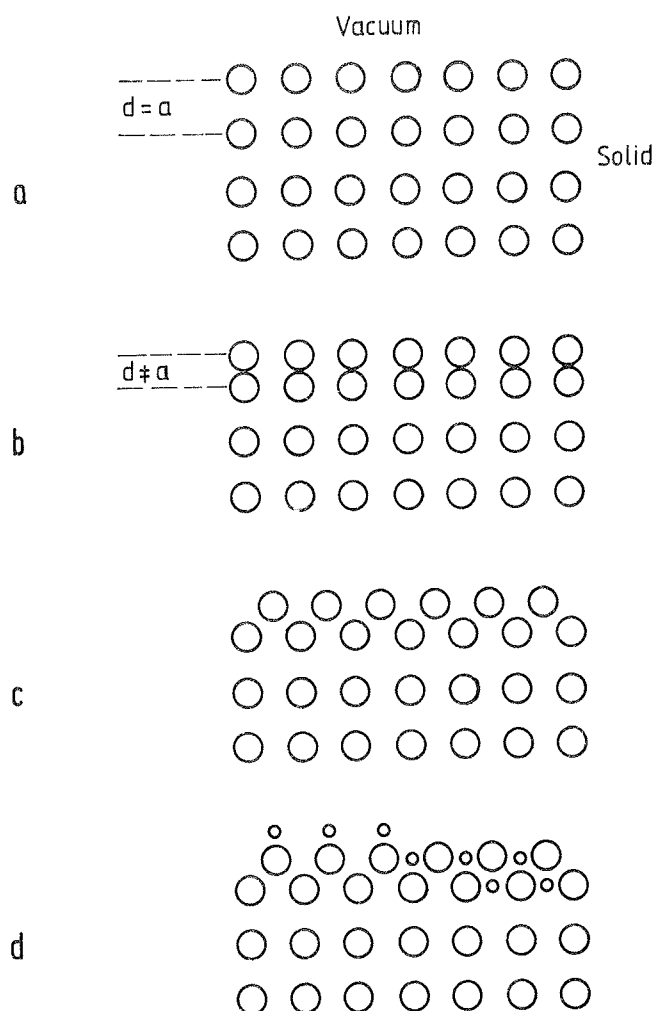


Fig. 1: Schematic of  
a) a solid surface created by terminating the bulk of a crystalline solid  
b) bonding imbalances cause the outer layer to move  
c) reconstruction of the surface  
d) when exposed to a reactive medium, foreign atom adsorption can occur, possibly leading to surface compound formation

forces at the surface leads to a rearrangement of the outermost atomic layers, fig. 1b, which may result in a relaxation or contraction up to 25% of the normal inter-layer spacing, as was shown by detailed structure analysis for several crystal planes of metals [1]. Surface reconstruction, fig. 1c, to minimize the surface energy, can occur and is observed for some crystal faces of covalently bonded semiconductor materials [2]. For surfaces which are exposed to reactive gas environment atomic adsorption followed by incorporation into the near surface region and surface compound formation can appear, fig. 1d.

For most real surfaces of polycrystalline materials the situation will be much more complex than for the ideal case of individual crystals as was discussed up to now. For polycrystalline materials not only the outer surface is of great importance, but also the structure and composition of inner interfaces like grain boundaries can drastically influence material properties, this is illustrated schematically in fig. 2. From all considerations up to now it can be concluded that the most important interface properties which have to be characterized by surface analytical methods are:

- the interface structure
- the chemical composition of the interface
- the chemical bonding state at the interface
- the electronic structure of the interface

To instrumentally probe a solid surface one of six basic probes may be applied to the surface: electrons, ions, neutrals, photons, heat or a field. The analysis consists of measuring the surface's response, also evident in one of these six ways, fig. 3. Combining all the probes and responses in principle a large number of experimental techniques results by which a surface may be analyzed.

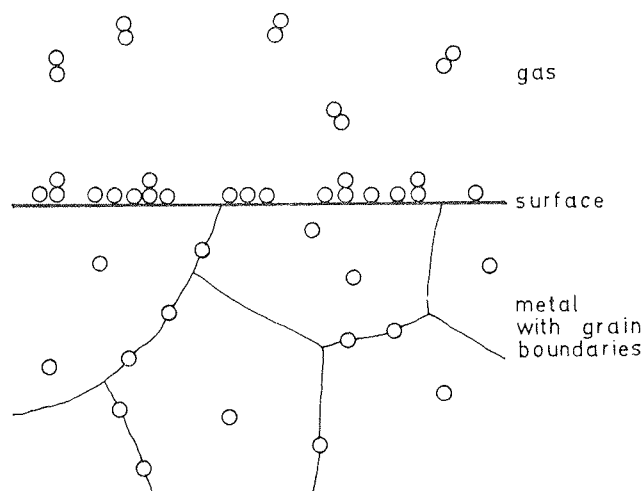


Fig. 2: Schematic of the equilibrium of species and nonmetal atoms (dissolved) in the metal matrix and segregated at the grain boundaries

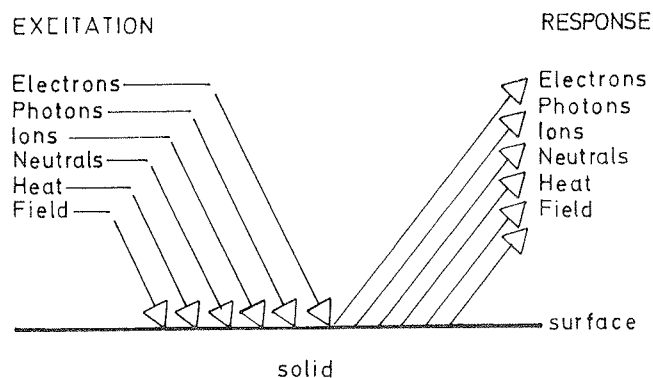


Fig. 3: Basic probes for surface analysis

Most of the standard surface analytical methods are based on unperturbed particle impact and detection and thus require vacuum conditions, where the mean free path of the gas molecules is larger than the dimensions of the reactor. Moreover, since it is demanded to analyze or characterize well-defined systems it is necessary to establish ultra high vacuum conditions. From kinetic gas theory it follows that the number of gas particles  $N_s$  striking a surface area of  $1 \text{ cm}^2$  per second is given by

$$N_s = N \sqrt{\frac{RT}{2\pi M}} = 2.634 \cdot 10^{22} \frac{p}{\sqrt{MT}}$$

where  $N$  equals the number of gas molecules per  $\text{cm}^3$  and  $p$  is the gas pressure in mbar. Assuming an average molecule is built of  $M = 28$  (which could be  $N$  or  $CO$ ) we can see that at  $10^{-6}$  mbar ambient pressure the number of particles colliding with  $1 \text{ cm}^2$  surface area is about  $10^{15}$  and corresponds to the average number of surface atoms being present in  $1 \text{ cm}^2$  surface area. So for a sticking coefficient of 1 within 1s a complete monolayer of gas molecules would cover the surface. Even at  $10^{-10}$  mbar still about  $10^{10}$  to  $10^{11}$  particles hit a  $1 \text{ cm}^2$  surface area in 1s, which means contamination problems could arise during long-term surface analysis.

The achievement of those necessary ultra high vacuum conditions nowadays is possible with commercial stainless steel vacuum chambers and for more detailed information relevant textbooks on vacuum technology exist [3-7].

### Experimental methods to characterize surfaces

During the last three decades a lot of different surface analytical methods (about 130) have been developed, but only a few of them have gained widespread use and will briefly be discussed here. These are:

- for structural analysis
  - LEED Low Energy Electron Diffraction
  - STM Scanning Tunneling Microscopy
- for the elemental composition and chemical bonding states
  - AES Auger Electron Spectroscopy
  - XPS X-ray Induced Photoelectron Spectroscopy
- for the elemental composition and/or for depth profiling
  - SIMS Secondary-Ion-Mass-Spectroscopy
  - SNMS Secondary-Neutrals-Mass-Spectroscopy

### LEED Low Energy Electron Diffraction

About 70 years ago the theoretically predicted wave nature of electrons [8] had been experimentally demonstrated by the LEED method [9]. According to the de Broglie relationship

$$\lambda = \frac{h}{p} \approx \frac{\sqrt{150}}{V} \text{ \AA}$$

an electron wave length  $\lambda$  may be derived from the momentum  $p$  and is related to the accelerating voltage  $V$  ( $\leq 1 \text{ keV}$ ) of an electron gun. Thus for electrons having a kinetic energy of 150 eV the wave length  $\lambda \approx 1 \text{ \AA}$  which is similar to the spacing between rows of atoms in a crystal. If on a well-ordered crystal surface mono-energetic electrons are impinging constructive interference occurs for elastically backscattered electrons depending on the crystal structure.

A schematic set-up of a LEED experiment is displayed in fig. 4. Low energy electrons are produced by a cathode and are focused on the sample. The backscattered electrons pass a grid system which cuts off the inelastically reflected electrons before the elastically diffracted electrons are post-accelerated on to a fluorescent screen. The diffraction and imaging process is illustrated by fig. 5. The sample crystal, characterized by the magnified two-dimensional grating, is mounted in the center of the screen curvature on a mechanical manipulator within a UHV chamber.

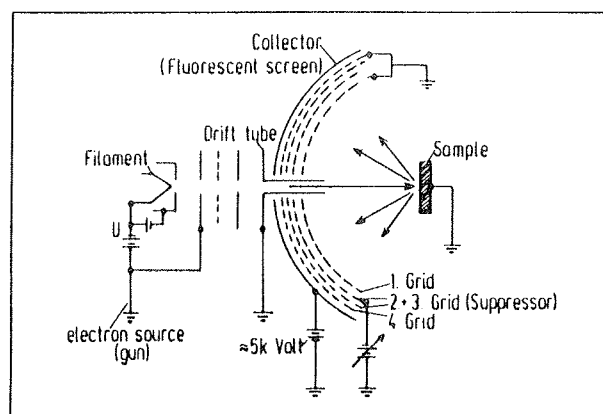


Fig. 4: Schematic set-up of a LEED experiment

The electron wave originating from the gun hits the surface and is diffracted at its atomic grating. The elastically backscattered electrons interfere with each other thus leading to diffraction maxima and minima. The maxima become visible on the fluorescent screen and characterize the surface ordering.

Fig. 6 gives a typical example, the diffraction pattern for a clean (100) oriented iron surface is shown.

If by an ordered surface reaction new positions on the clean surface will be occupied, additional reflexes on the fluorescent screen should appear if the ordering of the additional atoms is not related by a  $(1 \times 1)$  symmetry to the ordering of the surface atoms. The ordered enrichment of dissolved phosphorus atoms at higher temperature on (100) surface results at its saturation level in a so-called  $c(2 \times 2)$  surface structure, which is schematically demonstrated by fig. 7a. The corresponding LEED pattern registered for half a monolayer P atoms on the clean iron (100) surface is given in fig. 7b.

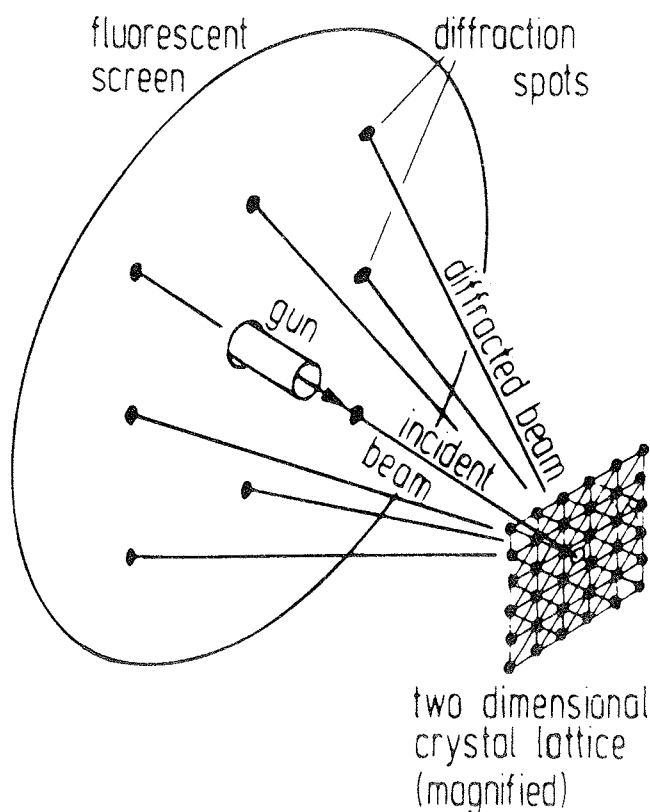


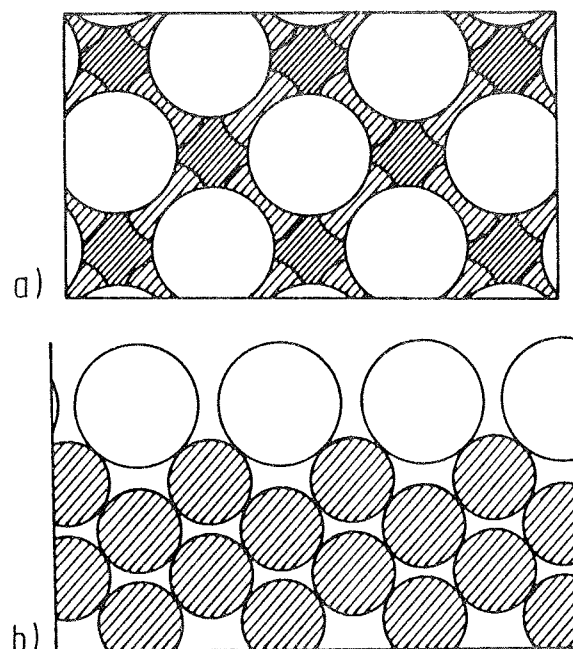
Fig. 5: Illustration of the diffraction and imaging process occurring on a surface with a two-dimensional grating



Fig. 6: First order LEED reflexes of a clean iron (100) surface

### The electron spectroscopic methods

Because of several principal and experimental similarities between the electron spectroscopic methods Auger Electron Spectroscopy (AES) and X-Ray Induced Photoelectron Spectroscopy (XPS), both methods will be discussed together. In both cases an electron energy analysis is performed with respect to electrons which are emitted from the sample under study after primary excitation with primary electrons in the case of AES and with X-Rays for XPS. For electrons which are emitted and traveling within a solid with a definite energy, the inelastic mean free path  $\lambda_M$  governs the surface sensitivity.  $\lambda_M$  is defined as the mean distance an electron travels before undergoing an inelastic event, i.e. some interac-



Model of  $c(2 \times 2)$  adsorption (segregation)

Fig. 7a: Schematic of a phosphorus  $c(2 \times 2)$  structure on an iron (100) surface

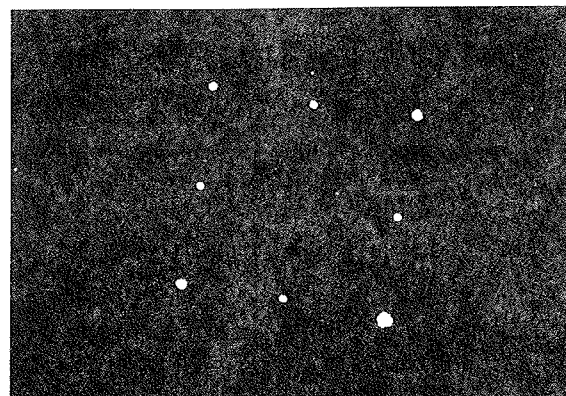


Fig. 7b: LEED pattern of a phosphorus  $c(2 \times 2)$  structure on Fe(100) (compare with fig. 6)

tion whereby it loses energy. A compilation of experimentally determined electron mean free path values for solid elements was given by Seah and Dench [10] and is displayed in fig. 8. For electrons within the range of 10-2000 eV, which is the typical energy range for the electron spectroscopic methods AES and XPS,  $\lambda_M$  is within the range of 0.5 to 2 nm or within about 2 to 10 atomic layers.

The actual escape depth  $\lambda$  of electrons depends on the direction in which they travel on their way to the analyzer:

$$\lambda = \lambda_M \cos \Theta$$

with  $\Theta$  being the emission angle with respect to the surface normal. Thus electrons emitted perpendicular to the surface will arise from maximum escape depth whereas electrons which are emitted nearly parallel to the surface come from the outermost region of the surface.

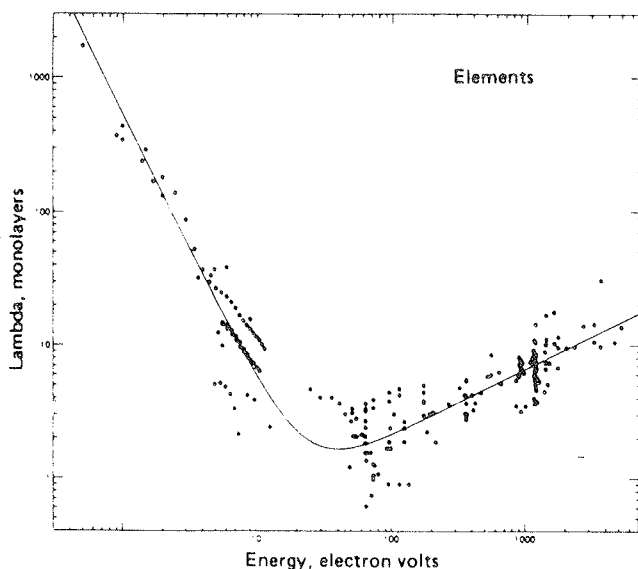


Fig. 8: Variation of the elastic mean free path for electrons in solids with energy after Seah and Dench /10/

By varying the angle of detection during an experiment the surface sensitivity may be enhanced for the electron spectroscopic methods.

The main components necessary to perform either Auger Electron Spectroscopy or Photo-electron Spectroscopy are very similar and fig. 9 gives a schematic representation of them. These consist of an excitation source (X-Ray source or electron gun), a sample/ support system, an electron energy analyzer and an electron detector (Multiplier), all maintained under ultra high vacuum. A further component outside the vacuum system are suitable electronics to convert the detected current into a readable spectrum. Two types of energy analyzers are currently most frequently in use, the cylindrical mirror analyzer (CMA), mainly for AES and the concentric hemispherical analyzer (CHA) mainly for XPS. Fig. 10 gives a schematic representation of both types of energy analyzers. More detailed information on the properties, advantages and disadvantages of the different analyzers may be found in literature /11/.

### Auger Electron Spectroscopy

The origin and nature of the Auger process /12/ can be understood from the schematic diagram of electron energy levels given in fig. 11. Ionizing radiation (electrons or X-Rays) ejects an electron from an atom in the solid, leaving a hole in one of the atomic core levels. This core level hole is quickly filled by an electron from a higher level and energy is released. This energy can be emitted in form of X-Rays or by a competing process where another electron gains energy and is ejected from the atom. This ejected electron is called an Auger electron and its energy depends on the energy of the atomic levels involved in its production and is independent of the energy of the ionizing radiation. Because of the

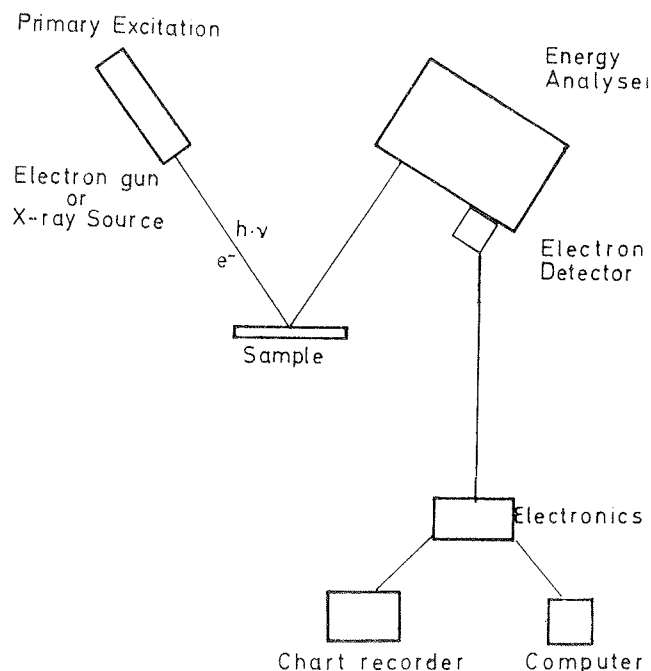


Fig. 9: Schematic representation of the components necessary for performing AES or XPS

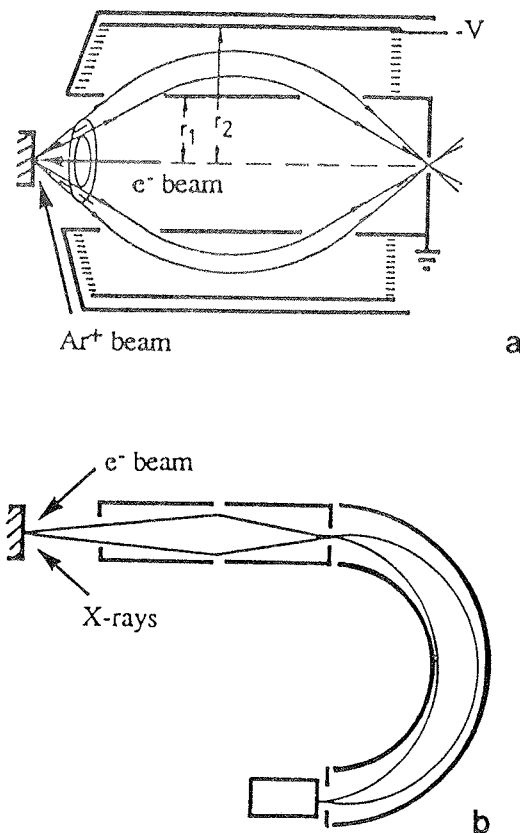


Fig. 10: Electron spectrometers used mainly for  
a) AES CMA Cylindrical mirror analyzer  
b) XPS CHA Concentric hemispherical analyzer

element specificity of the atomic energy levels, the emitted Auger electrons are element specific and the energy distribution of the emitted Auger electrons may therefore be used for an elemental analysis.

All elements besides H and He give rise to Auger electrons. For routine analysis of materials it is usually not necessary to understand the origin of the Auger transition in detail and as a first approximation the kinetic energy of an Auger electron may be given by (according to fig. 12)

$$E_{\text{kin}} = E_{L_1} - E_{L_{2,3}}$$

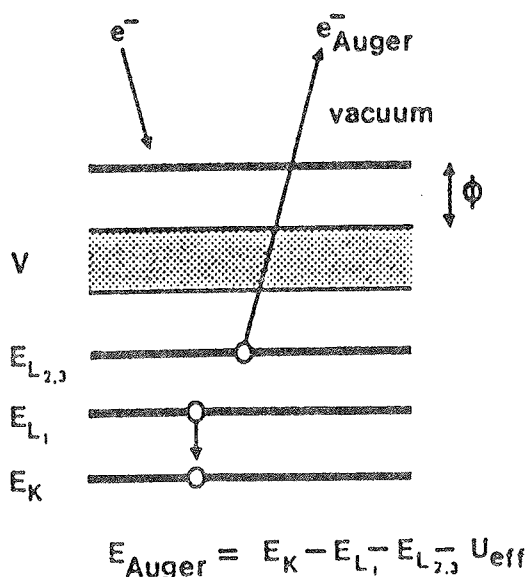


Fig. 11: Schematic of the Auger process

Auger spectra are normally displayed in one of two ways. The direct spectra, fig. 12a, which shows the energy distribution  $N \cdot N(E)$  in dependence on  $E$ . Historically however, the derivate spectra  $E \cdot (dN(E)/dE)$  have been preferred, fig. 12b, which has the advantage that the large slowly varying, inelastic background under the Auger peaks is suppressed, as may be recognized by a comparison of fig. 12a and 12b.

Auger spectra may be quantified with quite different levels of sophistication. The level of accuracy depends very much on the materials system and the instrument. Up to now there is no general method of quantifying Auger spectra. Several reviews on this subject are given in literature /13,14/.

### X-Ray Photoelectron Spectroscopy

Fig. 14 schematically presents the related process which is involved in the ejection of a photoelectron. The photoemission process is shown on an energy level diagram. The sample is irradiated with X-Rays of known energy  $h\nu$  and a sample electron is emitted from the K (or 1s) level. Due to the photoeffect the kinetic energy  $E_K$  of the emitted electron is given by

$$E_K = h \cdot \nu - E_B$$

where  $E_B$  is the binding energy of electrons in the K-level. As the energy  $h\nu$  of the X-Rays is known, a

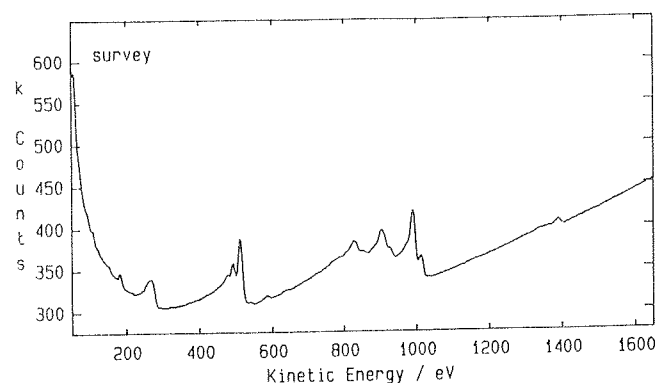


Fig. 12a: AES spectrum energy distribution  $N(E)/dE$  vs  $E$

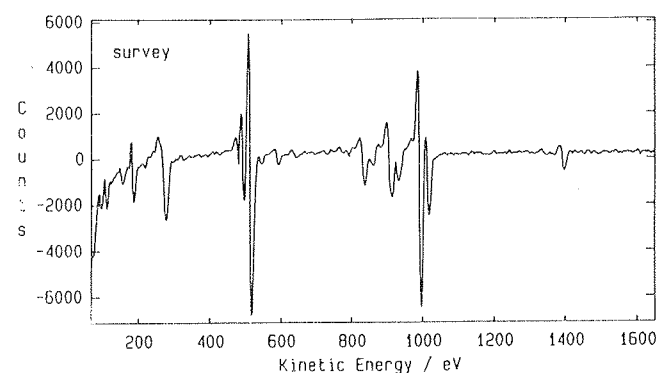


Fig. 12b: AES spectrum  $dN(E)/d(E)$  vs  $E$

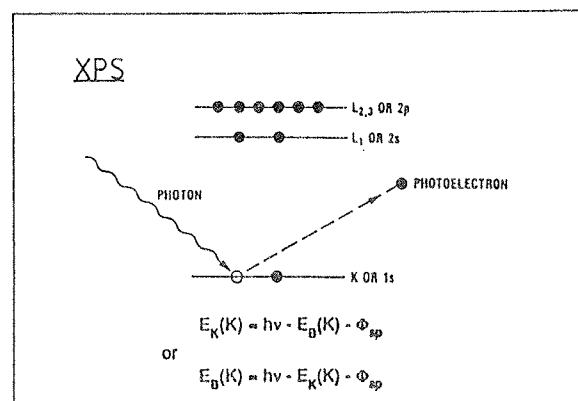


Fig. 13: Schematic representation of the XPS process

measurement of the kinetic energy of the photoelectron can be used to determine the binding energy of the electrons. A typical XP-spectrum is generated by plotting the measured photoelectron intensity as a function of binding energy, fig. 14. The binding energies of the observed lines are characteristic for each element and are a direct representation of the atomic orbital energies. Handbook data of these lines for all elements (besides H and He) exist /15/.

By XPS it is possible to distinguish between a particular element in different environments. This is due to the fact

that placing the same atom into different chemical environment gives rise to a change in the binding energies of the core-level electrons. This change in binding energy is called "chemical shift" and appears as a definite movement of the binding energy of the involved elemental peak in the XP-spectrum. One of the major advantages of XPS is the ease with which quantitative data can routinely be obtained. This is usually performed by determining the area under the peaks in question and applying previously determined sensitivity factors. A more detailed discussion of quantification of XPS results is given by several authors, for example by /16/.

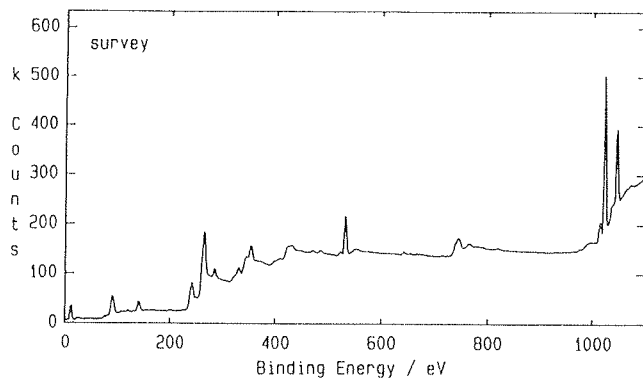


Fig. 14: XPS survey spectrum

As was pointed out already the depth from which photoelectrons are measured depends on the angle  $\Theta$  of detection, i.e. the angle of emission direction to surface normal, schematically shown in fig. 15. From this figure we can see that detection close the surface normal enhances signals from the bulk relative to the surface while detection close to the surface plane enhances the signal from the surface to the bulk. Thus by varying the angle of detection non-destructive depth information, as presented in fig. 16, can be achieved. This figure shows XPS data for a thin film of  $\text{SiO}_2$  on Si. For small values of  $\Theta$  the main contribution to the spectrum is from the bulk Si, while at larger values of the  $\Theta$  contribution from  $\text{SiO}_2$  becomes more important. For very thin layers on a substrate this approach is obviously preferable to the destructive ion etching methods for thin film analysis, which will be discussed in the following section.

### Secondary Ion Mass Spectrometry (SIMS)

The basic principle of the SIMS method is illustrated schematically in fig. 17. Primary ions of high enough energy (0.1 to 10.0 keV) bombard the surface of a solid and generate a collision cascade within the surface near region of the sample. During this impact ionized atomic or molecular species are emitted from the surface into the vacuum. The ejected secondary ions are detected by a mass spectrometer. The distribution of the emitted positive and negative ions is characteristic for the chemical composition of the sample surface. There are two

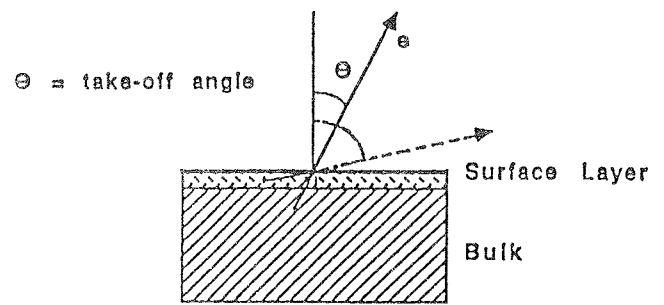


Fig. 15: Schematic showing surface sensitivity as a function of emission angle. Small  $\Theta$  enhances the signal from the bulk, while large  $\Theta$  enhances the signal from the surface

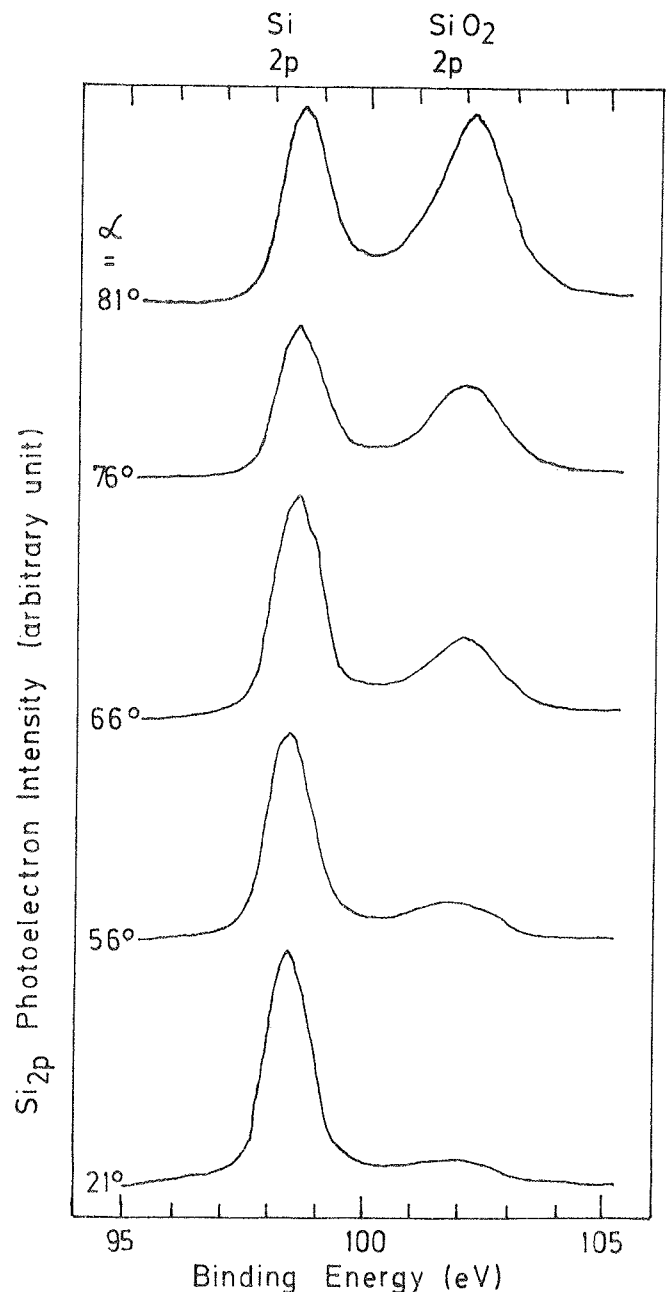


Fig. 16: Study by XPS of the interface between Si and a thin film of  $\text{SiO}_2$  on the Si substrate.  $\alpha$  - angle between surface and normal

different modes of application of the SIMS method. For the static SIMS method very low primary ion current densities are used so that the analysis is restricted to the outermost atomic layer of the solid sample. If fine focused ion sources are used and the primary ion beam is scanned across some sample area, the secondary electrons emitted by the impact cascade may be used to get a topographic image of the sample. By recording selected emitted secondary ions, an elemental mapping of the sample surface is possible. Each elemental mapping of the sample surface is possible. Each elemental corresponds to one removed atomic layer.

For the dynamic SIMS method high ion beam current densities are used in order to sputter with a relatively high rate succeeding surface layers. By this a high detection sensitivity of  $10^{13}$  atoms per  $\text{cm}^3$  can be reached. This high sensitivity combined with the possibility to measure concentration profiles means that this kind of application of SIMS is ideal to determine doping and impurity levels in solids. By SIMS not only all elements but also isotopes can be detected mass spectrometrically.

A schematic drawing of a SIMS system is given in fig. 18. The main components are the ion source, the mass spectrometer and the sample holder and manipulator. Additionally, an electron gun may be used for charge compensation during analysis of poor conducting samples or insulators. The oxygen ion source enables reactive sputtering in order to increase the secondary ion

yield for metallic samples and to minimize so-called matrix effects.

The static method of SIMS was very frequently used to study the adsorption of gases particularly oxygen on metal surfaces. To illustrate the possibilities of the static SIMS method an example will be given for carbon monoxide adsorption on an iron surface. Depending on the kind of metal the adsorption of carbon monoxide on metal surfaces may be molecular or dissociative. Examples are

Cu, Pd, Ni molecular  
and W dissociative

In the case of iron both types of carbon monoxide adsorption can occur. By static SIMS studies the individual type of adsorption may be characterized by the type of secondary ions which appear during sputtering as was shown by /17/ for example for CO adsorption on iron, fig. 19. For dissociative adsorption  $\text{MC}^+$ ,  $\text{MO}^+$ ,  $\text{MO}_2^+$  and  $\text{M}_2\text{C}^+$  (M for metal) secondary ions should be observed and on the other hand molecular adsorption. Fig. 19 demonstrates that for CO adsorption on iron all types of secondary ions were registered.

### Secondary Neutrals Mass Spectrometry (SNMS)

The SNMS method shows many similarities with the SIMS method discussed before. Again primary ions of

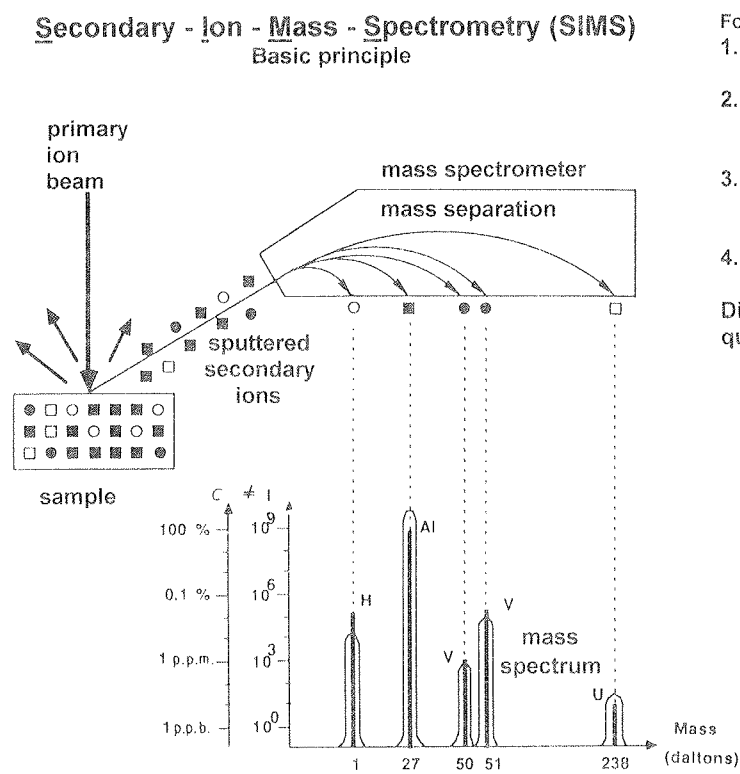


Fig. 17: Schematic of the SIMS process

Four steps are involved in SIMS characterisation:

1. The bombardment of the sample (under uhv-conditions) by primary ions of sufficient energy in the keV range
2. Sputtering of the outermost atomic layers, the sputtered material consists of about 99% secondary neutrals and a small fraction of positive or negative secondary ions
3. The extraction of the emitted ions prior to their injection into a mass spectrometer which separates (or filters) the different species according to their mass/charge ratio
4. The detection of the secondary ions with a large dynamic range ( $10^{10}$ ) in intensity I (c.p.s.)

Different types of mass spectrometers can be used: quadrupoles, ToF, magnetic.



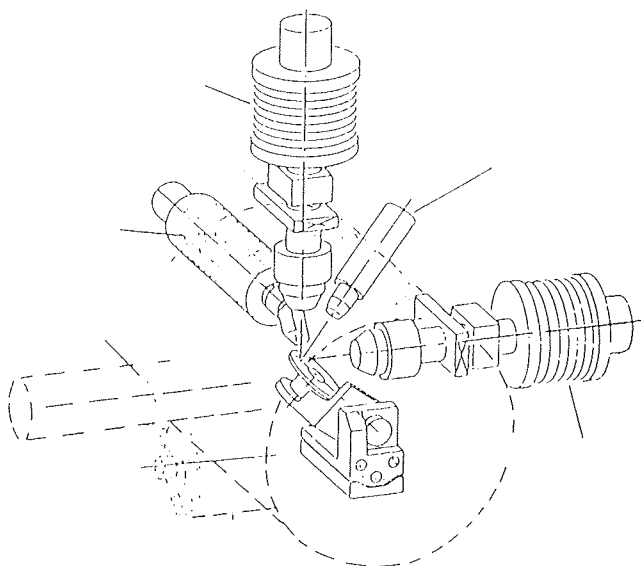


Fig. 18: SIMS system (main components)

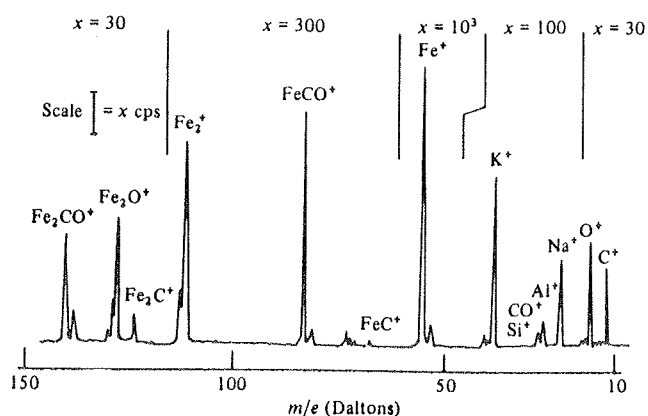


Fig. 19: SIMS spectrum recorded at equilibrium when iron is exposed to  $10^{-8}$  Torr of carbon monoxide

high enough energy (0.1 to 10 keV) generate a collision cascade in the surface near region of a solid sample. As a consequence molecular and atomic fragments are emitted from the surface into the vacuum. The emitted secondary ions used for SIMS analysis are separated and the emitted neutrals are post ionized by electron impact and detected by a mass spectrometer. Also in this case the emitted neutrals are characteristic for the chemical composition of the sample surface. Post ionization may also be performed by a low pressure plasma above the sample or by laser bombardment. Decoupling the sputter and ionization process the ionization probabilities are predictable and independent on matrix effects. For this reason, the SNMS method is much better suited for quantitative measurements than the SIMS method.

## References

- /1/ M.A. Van Hove, S.Y. Tong, Surface Crystallography by LEED, Berlin: Springer Ser. Chem Phys. Vol. 2, 1979
- /2/ J.B. Pendry, Low Energy Electron Diffraction, London: Academic, 1974
- /3/ E.A. Trendelenburg, Ultrahochvakuum, Karlsruhe: Braun, 1963
- /4/ S. Dushman, J.M. Lafferty, Scientific Foundations of Vacuum Technique, New York: Wiley, 2nd edn., 1962
- /5/ C. Edelmann, H.G. Schneider, Vakuumpophysik und -technik, Leipzig: Akademische Verlagsgesellschaft Geest und Portig, 1978
- /6/ P.A. Readhead, J.P. Hobson, E.V. Kornelsen, The Physical Basis of Ultrahigh Vacuum, London: Chapman and Hall, 1968
- /7/ N.W. Robinson, The Physical Principles of Ultrahigh Vacuum Systems and Equipment, London: Chapman and Hall, 1968
- /8/ L. de Broglie, Phil. Mag. 47, 446, 1924
- /9/ C.J. Davisson and L.H. Germer, Proc. Natl. Acad. Sci. US 14
- /10/ M.P. Seah, W.A. Dench, Surf. Interface Anal. 1(2), 1979
- /11/ C.R. Brundle, A.D. Baker, "Electron Spectroscopy", New York: Academic Press, 1982
- /12/ P. Auger, "Sur L'Effect Photoélectrique Composé", J. Phys. Radium, 6, p. 205, 1925
- /13/ D. Briggs, M.P. Seah, Practical Surface Analysis. New York: John Wiley, 1983
- /14/ C.J. Powell, Quantitative Surface Analysis of Materials. ASTM STP 643, 1978
- /15/ C.D. Wagner, W.M. Riggs, L.E. Davis, J.F. Moulder, G.E. Muilenberg, Handbook of X-Ray Photoelectron Spectroscopy. Perkin Elmer Corp. Physical Electronics Div., 6509 Flying Cloud Drive, Eden Prairie Minnesota 55344, USA
- /16/ E.G. Briggs, Handbook of X-Ray and Ultraviolet Photoelectron Spectroscopy. Heyden and Sons, 1977
- /17/ A. Benninghoven, F.G. Ruedenaver, H.W. Werner, Secondary Ion Mass Spectrometry, New York: Wiley, 1987

H. Viefhaus  
Max-Planck-Institut für Eisenforschung GmbH  
Max-Planck-Str. 1  
D-40237 Düsseldorf, Germany  
tel. + 49 211 6792 290  
fax + 49 211 6792 268

Prispelo (Arrived): 29.9.1994

Sprejeto (Accepted): 22.11.1994